View Article Online
View Journal

Green Chemistry

Cutting-edge research for a greener sustainable future

Accepted Manuscript

This article can be cited before page numbers have been issued, to do this please use: H. Li, X. Ding and T. Zhou, *Green Chem.*, 2026, DOI: 10.1039/D6GC02196D.

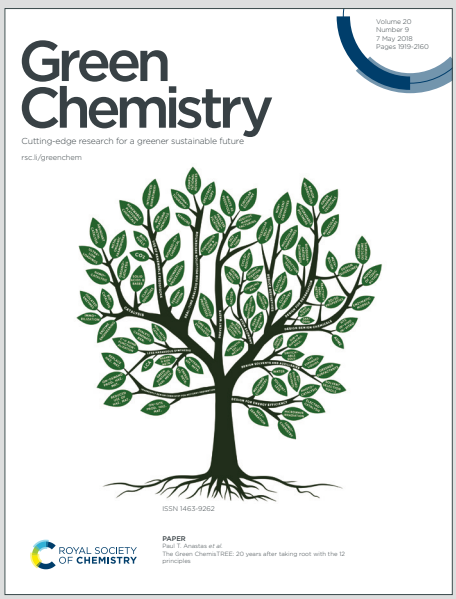

View Article Online
DOI: 10.1039/D6GC02196D

Green Foundation

1. This work advances green chemistry by large-scale screening (from 2,562 candidates) and replacing the reprotoxic cosolvent NMP in water-lean solvents with eco-friendly alternatives for CO_2 capture.

2. The developed solvent EM-A-5H delivers a cyclic capacity of 0.86 mol CO_2/mol amine, 93.6% regeneration efficiency, and a total regeneration energy of 2.20 GJ/t CO_2, which is 41% lower than 30 wt% MEA and 15% lower than its NMP-based counterpart. It also maintained high stability over multiple absorption–desorption cycles without performance degradation. In summary, this new water-lean solvent not only addresses toxicity issues but also achieves superior CO_2 capture performance.

3. Further greening can be achieved by optimizing water content and viscosity, quantifying solvent loss, degradation, and corrosion, and conducting life-cycle assessments under realistic operating conditions.

View Article Online
DOI: 10.1039/D6GC02196D

ARTICLE

Greening Water-Lean Solvents for CO_2 Capture: Replacing Toxic 1-Methyl-2-pyrrolidone with High-Performance Eco-Friendly Cosolvents

Received 00th January 20xx,
Accepted 00th January 20xx

DOI: 10.1039/x0xx00000x

Huilin Li [a], Xuechong Ding [a] and Teng Zhou *[a,b]

Water-lean solvents are promising alternatives to aqueous amines for post-combustion CO_2 capture due to their lower regeneration energy. However, the majority of state-of-the-art water-lean solvents rely on 1-methyl-2-pyrrolidone (NMP) as the organic cosolvent, whose reproductive toxicity poses a serious barrier to large-scale deployment. This study proposes a systematic strategy to identify green, low-toxicity replacements for NMP in water-lean solvents. Based on COSMO-RS σ-profile similarity calculation, 20 high-potential candidates were first identified from 2,562 organic solvents. Subsequent environmental, health, and safety (EHS) evaluations, combined with physicochemical property filtering, narrowed the selection to two green cosolvents: methylaminoacetaldehyde dimethyl acetal (MAADMA) and 3-methoxy-1-butanol (MOB). These two candidates and NMP were then experimentally validated in combination with three representative amines (EMEA, DMEDA, and DMPDA) at 5 wt% water content. Among all tested systems, the EM-A-5H solvent (30% EMEA / 65% MAADMA / 5% H_2O) showed the best performance, with a remarkable cyclic capacity of 0.86 mol CO_2/mol amine and a regeneration efficiency of 93.6%. Importantly, EM-A-5H achieved a total regeneration energy of 2.20 GJ/t CO_2, 41% lower than conventional 30 wt% MEA and 15% lower than the NMP-based counterpart solvent. It also exhibited an excellent stability and satisfactory viscosity over seven absorption–desorption cycles without performance degradation. This work offers a systematic and practical approach for the rational design of eco-friendly, high-performance water-lean solvents for CO_2 capture.

Introduction

The transition toward greener and safer solvent systems has become a central theme in modern chemical engineering and industrial chemistry[1-5]. This trend has profoundly influenced fields, such as pharmaceuticals[6,7], fine chemicals[7,8], and separation engineering[9,10], and is increasingly reshaping solvent design in carbon capture technologies as well[11,12].

Among the available CO_2 capture routes, post-combustion capture by chemical absorption remains one of the most mature and industrially relevant technologies[13] because of its high capture efficiency and technical readiness. However, conventional aqueous amine systems still suffer from several well-recognised drawbacks, including high regeneration energy demand[14], solvent degradation[15,16] and corrosion[17].

The development of advanced solvent systems for CO_2 capture has been gradually shifted from conventional aqueous amines[18,19] to non-conventional solvents[20-25]. Recently, water-lean solvents have garnered tremendous attention from both academia and industry. By replacing a significant portion of water with organic cosolvents, water-lean systems not only drastically reduce the specific heat capacity of the solution but also lower the energy penalty associated with solvent vaporization in the regeneration step.

In practice, the performance of water-lean solvents is still constrained by the trade-off among CO_2 capacity, viscosity, and regeneration behaviour. At present, most of the better-performing water-lean solvents rely on 1-methyl-2-pyrrolidone (NMP) as a cosolvent. Xu et al.[26,27] developed an N,N-dimethyl-1,2-ethanediamine (DMEDA)/NMP system, which exhibited a 140% higher CO_2 cyclic capacity, a 42% lower regeneration heat, and a 37% higher absorption rate than 30 wt% monoethanolamine (MEA). Qi et al[28] proposed a 2-(ethylamino)ethanol (EMEA)/NMP solvent that delivered a 69% lower regeneration duty than that of MEA in bench-scale experiments. Liu et al.[29] further demonstrated in a pilot-scale test that EMEA/NMP again achieved a 43% lower regeneration energy, together with 30% and 60% faster absorption and desorption kinetics, respectively. Moreover, Zhu et al.[30] showed that 3-dimethylaminopropylamine (DMPDA)/NMP exhibited a 58% reduction in regeneration heat compared to MEA. Overall, previous studies consistently show that incorporating NMP is beneficial for improving the overall performance of water-lean solvents. However, the toxicological concerns associated with NMP, particularly its reproductive toxicity, are well recognized

[a] Sustainable Energy and Environment Thrust, The Hong Kong University of Science and Technology (Guangzhou), Nansha, Guangzhou 511400, China
[b] Department of Chemical and Biological Engineering, The Hong Kong University of Science and Technology, Hong Kong SAR, China
* Corresponding author: tengzhou@hkust-gz.edu.cn

and difficult to reconcile with the growing demand for safer and more sustainable solvent systems[31]. Consequently, replacing toxic cosolvents such as NMP with greener alternatives has become both a necessary and timely direction for the further development of water-lean CO_2 absorbents.

An ideal green organic solvent should not only exhibit lower toxicity and improved environmental compatibility but also preserve or enhance the key merits of water-lean absorbents, including high CO_2 uptake, fast absorption kinetics, and favourable regeneration characteristics. However, there is still a lack of studies specifically addressing the replacement of toxic organic solvents in water-lean absorbents. Conventional trial-and-error approaches frequently encounter a dilemma: molecules with substantial structural deviations often lack sufficient solvation capability, whereas structural analogues tend to exhibit similar toxicities.

In the present work, we investigate the feasibility of employing green organic solvents as substitutes for conventional toxic cosolvent in water-lean solvents. The aim is to evaluate whether solvent greenness can be improved without sacrificing the thermodynamic and kinetic advantages of water-lean solvent systems. Green solvent candidates were first systematically screened from a database of 2,562 organic solvents. Their absorption performance, desorption behaviour, and regeneration energy were then comprehensively evaluated, followed by cyclic experiments to assess their operational stability. In addition, viscosity was measured, and solvent cost and operability were also assessed to examine the practical applicability of the identified green solvent. Based on these results, this work seeks not only to demonstrate the absorption and regeneration advantages of a novel green solvent candidate but also to provide practical guidance for the development of environmentally friendly, low-toxicity water-lean solvents for CO_2 capture.

Methods

Computational Solvent Screening

Combining quantum chemical information with statistical thermodynamics, Conductor-like Screening Model for Real Solvents (COSMO-RS) has emerged as an essential tool for predicting the thermodynamic properties and non-ideal behaviours of fluid phases[32,33]. In this study, computational solvent screening was performed using the COSMO-RS model.

Based on high-precision quantum chemical calculations, the screening charge density (σ) on the molecular surface is transformed into a probability distribution function in statistical thermodynamics, known as the σ-profile, P(σ)[34,35]. This profile quantitatively delineates the hydrogen-bond donor capacity, hydrogen-bond acceptor capacity, and non-polar characteristics of a molecule, strongly determining its pseudo-chemical potential and activity coefficient in a given solvent. Consequently, the σ-profile serves as a thermodynamic electrostatic fingerprint that dictates the macroscopic solvation behaviour of a molecule.

To identify a green alternative to the reprotoxic solvent NMP, we established an automated screening strategy based on electrostatic feature similarity. In this work, the σ-profile (one type of charge density distribution) of each solvent was represented as a discrete vector over the σ range from −0.035 to +0.035 e·Å^{-2} with a bin interval of 0.001 e·Å^{-2}. The similarity between each candidate molecule and the benchmark solvent NMP was then calculated using the cosine similarity metric[36], a widely adopted approach for molecular similarity comparison[37]. Molecules with a higher similarity index are more likely to exhibit dissolution and phase-regulation properties similar to those of NMP in water-lean amine-based CO_2 capture systems[38]. Using this approach, the algorithm extracted the 20 high-potential molecules with a similarity score exceeding 98% from a database of 2,562 organic solvents. These molecules formed the candidate pool for subsequent environmental, health, and safety (EHS) assessments, along with the evaluation of two other key physicochemical properties, to further screen practical solvents.

EHS and property screening

A systematic EHS assessment was subsequently conducted for the pre-selected top 20 candidates using the comprehensive CHEM21 solvent selection guide[39,40]. The CHEM21 framework rigorously evaluates solvents across three primary criteria: environment (E), health (H), and safety (S). To quantify the hazard level, each criterion is assigned a discrete score ranging from 1 to 10, where 10 represents the highest hazard. The final ranking of a solvent into "Recommended", "Problematic", or "Hazardous" strictly depends on the combination of these three scores.

Rather than using an additive total, the CHEM21 framework employs a strict threshold-based system to ensure that no single severe EHS hazard is overlooked:

- Hazardous: Any single criterion with a score ≥ 8, or at least two criteria with score ≥ 7.
- Problematic: Exactly one criterion with a score of 7, or at least two criteria falling within the yellow tier (scores 4–6).
- Recommended: All other combinations.

In this study, to genuinely overcome the reprotoxic limitation of the benchmark solvent NMP, only solvents with an overall “Recommended” green status were considered for further screening. To further streamline solvent development and enhance engineering applicability, boiling point (BP) and hydrophobicity (LogP) were introduced as additional selection criteria. Organic solvents with excessively low boiling points were considered unsuitable because high volatility could lead to solvent loss and compromise process stability during CO_2 capture. Meanwhile, LogP was included as an indicator of phase behaviour, since lower values are generally associated with a

lower tendency toward phase separation during CO_2 absorption[41,42].

Therefore, only solvents that simultaneously satisfied all three conditions, an overall "Recommended" green status, a boiling point above the typical absorber temperature range (373−393 K), and a LogP below 1.0, were selected for the final carbon capture performance validation stage.

Experimental section

Chemicals

Gaseous carbon dioxide (CO_2, 99.999%) and nitrogen (N_2, 99.9%) were supplied by Guangzhou Guangqi Gas Co., Ltd. Concentrated sulfuric acid (H_2SO_4) was purchased from Guangzhou Chemical Reagent Factory, China. All amines and organic solvents used in this study were procured from Shanghai Aladdin Industrial Co., China, including monoethanolamine (MEA, 99%), 2-(ethylamino)ethanol (EMEA, 99%), N,N-dimethyl-1,2-ethanediamine (DMEDA, ≥98%), N,N-dimethyl-1,3-propanediamine (DMPDA, ≥99%), 1-methyl-2-pyrrolidone (NMP, ≥99%), methylaminoacetaldehyde dimethyl acetal (MAADMA, 97%), and 3-methoxy-1-butanol (MOB, ≥99%). All chemicals were used as received. Deionized water was used to prepare the water-lean solutions.

Phase behaviour

To systematically evaluate the macroscopic phase stability of the screened candidates, a continuous CO_2 bubbling test was conducted. For each test, 15 mL of freshly prepared water-lean amine solution was transferred into a transparent glass vial. Pure CO_2 gas with a flow rate of 50 mL/min was continuously introduced into the liquid phase. The absorption process was maintained for up to 48 hours at 313 K in a constant temperature water bath (LC-WB-1, ± 1 K, Lichen).

Throughout this prolonged CO_2 loading period, the macroscopic state of the solution was visually inspected every 12 hours. After CO_2 absorption, the solvent behaviour was classified into four categories: homogeneous, biphasic, gelation, and crystallization. These were assigned according to the following criteria. Homogeneous was defined as a single transparent liquid phase without visible turbidity, solid particles, or a liquid–liquid interface. Biphasic separation was defined as the formation of two liquid phases with a clear liquid–liquid interface. Gelation was identified by the loss of macroscopic fluidity with no discrete crystalline particles observed. Crystallization was assigned when visible solid particles or crystals appeared in the liquid phase or on the vial wall. Solvents exhibiting biphasic separation, gelation, or crystallization were immediately discarded.

Absorption and desorption

The dynamic absorption and desorption performance was evaluated under a CO_2 partial pressure of 12 kPa (simulated flue gas) using the experimental setup shown in Figure 1. The system consists of a temperature control unit (GTZL-2C25V, ± 0.5 K, Guante), a 500 mL reactor equipped with a mechanical agitator (AC500, ± 1 r/min, SenLong), a mass flow controller (D07-11C, ± 1.5% accuracy, Seven Star), and a cooling condenser (T-300, ± 1 K, BiLon).

Before each test, 150 mL of fresh solvent was introduced into the reactor, purged with N_2 at 100 mL/min for 1 hour, and heated to 313 K. Once stabilized, a simulated flue gas (12 kPa CO_2 balanced with N_2) was injected at a flow rate of 500 mL/min under agitation at 500 r/min. After absorption, 500 mL/min of N_2 was employed to the desorption process. The outlet CO_2 concentration was continuously monitored using an online infrared gas analyser (GXH-3011N, ≤ 0.4%, Huayun). To ensure consistent comparison across all solvents, the absorption and desorption durations were set to 250 min and 300 min, respectively. Additionally, to determine the maximum CO_2 absorption capacity under a CO_2 partial pressure of 12 kPa, experiments were conducted using the same setup described above. After saturation, the equilibrium CO_2 loading was quantified using a Chittick apparatus following the method described by Dreimanis[43].

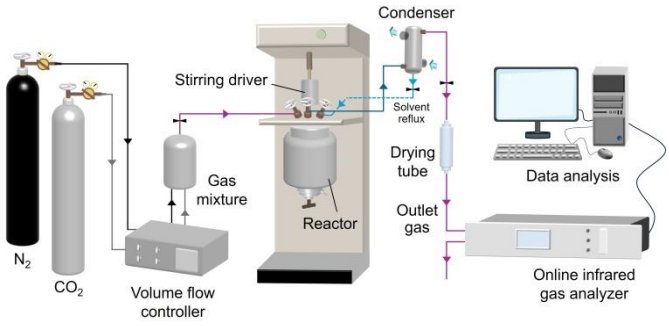

Figure 1. Schematic diagram of the cyclic absorption–desorption apparatus

Regeneration energy

The total regeneration energy (Q_{reg}, GJ/t CO_2) consists of three primary components: the heat of absorption or reaction (Q_{rea}), sensible heat (Q_{sen}) and latent heat (Q_{lat}), as shown in Eq. (1). The detailed calculation for each term is given in Eq. (2).

$$Q_{reg} = Q_{rea} + Q_{sen} + Q_{lat} \quad (1)$$

$$Q_{reg} = \frac{-\Delta H_{abs}}{M_{CO_2}} + \frac{c_p m_{sol} \Delta T}{m_{CO_2}} + \frac{n_{H_2O}}{M_{CO_2} n_{CO_2}} \Delta H_{H_2O}^{vap} \quad (2)$$

where ΔH_{abs} is the heat of absorption (kJ/mol CO_2), M_{CO_2} is the molecular weight of CO_2 (g/mol), c_p is the heat capacity of solvent (kJ·kg^{-1}·K^{-1}), m_{sol} is the mass of the solvent (kg), ΔT represents the effective temperature difference for sensible heating, determined by the heat exchanger approach, set to 10 K in this work. m_{CO_2} is the mass of CO_2 absorbed (g), n_{H_2O} is the amount of water

evaporated during desorption (mol), n_{CO_2} is the amount of CO_2 desorbed (mol), and $\Delta H_{H_2O}^{vap}$ is the heat of water evaporation at 353 K (41.59 kJ/mol).

Both the heat of absorption and heat capacity of the solvent were directly measured using a microcalorimeter (CALVET 80, ± 0.1% accuracy, Setaram). To determine n_{H_2O} and n_{CO_2}, after absorption, 60 g of each CO_2-rich solvent was transferred into the desorption apparatus shown in Figure 2. This solvent was desorbed in a thermostatic magnetic stirring oil bath (MS-H220-V3, ± 1 K, DLAB) at 353 K for 300 min, with the stirring rate maintained at 800 rpm. Water vapor generated during desorption was condensed and collected using a condenser. Based on the mass of the collected condensed water and the CO_2 loadings (using the Chittick apparatus, Dreimanis[43]) of the solvent before and after desorption, n_{H_2O} and n_{CO_2} were determined, respectively.

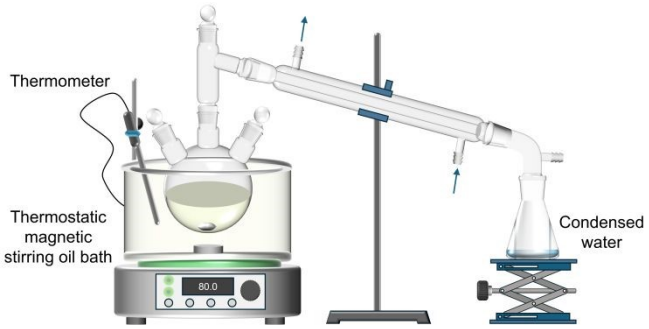

Figure 2. Apparatus to measure the amount of evaporated water during the desorption step

Solvent stability

Investigating the antioxidant and degradation stability is critical for maintaining long-term solvent performance and extending the service life of solvents in practical applications. The cyclic stability of the identified green water-lean solvent was evaluated by continuous absorption–desorption experiments using the same apparatus as shown in Figure 1. The absorption step was carried out at 313 K for 250 min, followed by desorption at 353 K for 300 min. All other operating conditions were consistent with those described previously.

Viscosity measurement

Solvent viscosity is a critical parameter for gas absorption because it affects absorption and desorption rates, diffusion resistance, pumping energy, and column hydrodynamics. The viscosity of the identified green water-lean solvent was measured at different CO_2 loadings at 313 K using a rotational viscometer (ViscoQC 300, ± 1.0% accuracy, Anton Paar, Austria) equipped with a Peltier temperature control device (PTD 80, ± 0.1 K, Anton Paar, Austria).

Results and discussion

Green solvent screening

By evaluating the σ-profile similarity to NMP, the top 20 potential solvent candidates were identified from a comprehensive database of 2,562 organic solvents. These candidates were subsequently subjected to an EHS assessment to verify their greenness, as presented in Table 1.

All these candidates exhibited a similarity score exceeding 98%, indicating highly comparable polarity and hydrogen-bonding characteristics to those of the benchmark solvent NMP. However, the majority of them failed to meet the sustainability criteria. Specifically, five solvents were classified as "Hazardous", the same category as the benchmark solvent NMP. This group included structural analogues such as 1,3-dimethyl-2-imidazolidinone, 2-pyrrolidone, and 2,5,8,11-tetraoxadodecane, all of which exhibited severe health and environment risks. Eleven additional candidates were classified as “Problematic”, primarily due to their poor environmental performance.

Consequently, by strictly adhering to the green threshold, these 16 candidates were excluded. Only four solvents within the category of “Recommended” met the criterion. They are methylaminoacetaldehyde dimethyl acetal (Rank 9), diethyl dimethylamidophosphate (Rank 12), 3-methyl-2-cyclohexen-1-one (Rank 13), and 3-methoxy-1-butanol (Rank 16).

To finalize the selection for experimental validation, the engineering suitability of the four recommended solvents was critically assessed (Table 2). While candidates 12 and 13 exhibited high boiling points indicating good thermal stability, their pronounced hydrophobicity strongly deviated from the desired hydrophilic nature required to maintain a stable, homogeneous water-lean amine blend, suggesting a potential risk of phase separation. In contrast, candidates 9 and 16 possessed highly compatible LogP values of 0.21 and −0.02, respectively, ensuring excellent phase stability, alongside sufficiently high boiling points. Consequently, these two solvents were selected as the optimal green replacements and advanced to the subsequent experimental stage for comprehensive CO_2 absorption and desorption performance validation.

View Article Online
DOI: 10.1039/D6GC02196D

Table 1. σ-profile similarity and CHEM21-based EHS evaluation of the top 20 solvent candidates.

Rank	Solvent	CAS No.	Similarity	Safety Score	Health Score	Environ. Score	Classification
N.A.	N-methyl-2-pyrrolidinone (NMP)	872-50-4	100.00%	1	9	7	Hazardous
1	1,3-dimethyl-2-imidazolidinone	80-73-9	99.49%	1	9	7	Hazardous
2	2,2'-(methylimino)bis-ethanol	105-59-9	99.17%	1	2	7	Problematic
3	2,5-dimethoxytetrahydrofuran	696-59-3	99.02%	3	6	5	Problematic
4	2-pyrrolidone	616-45-5	98.92%	1	9	7	Hazardous
5	4-(2-hydroxyethyl)morpholine	622-40-2	98.91%	1	2	7	Problematic
6	2-piperidinone	675-20-7	98.83%	1	2	7	Problematic
7	Diethylene glycol monoethyl ether	111-90-0	98.78%	1	2	7	Problematic
8	N,N-bis(2-hydroxyethyl) ethylamine	139-87-7	98.78%	1	2	7	Problematic
9	**Methylaminoacetaldehyde dimethyl acetal**	**122-07-6**	**98.66%**	**3**	**1**	**5**	**Recommended**
10	1,1-dimethoxyethane	534-15-6	98.58%	5	3	5	Problematic
11	Triethanolamine	102-71-6	98.53%	1	1	7	Problematic
12	**Diethyl dimethylamidophosphate**	**2404-03-7**	**98.47%**	**1**	**2**	**5**	**Recommended**
13	**3-methyl-2-cyclohexen-1-one**	**1193-18-6**	**98.42%**	**1**	**2**	**5**	**Recommended**
14	Tetramethylurea	632-22-4	98.35%	1	6	5	Problematic
15	1,2-dimethoxyethane	110-71-4	98.33%	6	9	3	Hazardous
16	**3-methoxy-1-butanol**	**2517-43-3**	**98.32%**	**3**	**1**	**5**	**Recommended**
17	Tripropyleneglycol	24800-44-0	98.32%	1	1	7	Problematic
18	2,5,8,11-tetraoxadodecane	112-49-2	98.28%	N.A.	9	7	Hazardous
19	2-methoxyethanol	109-86-4	98.17%	3	9	3	Hazardous
20	Triethyl phosphate	78-40-0	98.11%	1	2	7	Problematic

Table 2. Key physicochemical properties of NMP and four recommended green solvents.

Rank (abbr.)	MW (g·mol^{-1})	BP (℃)	LogP
NMP	99.13	202.0	−0.38
9 (MAADMA)	119.16	140.0	0.21
12	181.17	193.5	1.73
13	110.15	199.0	1.04
16 (MOB)	104.15	162.6	−0.02

Phase behaviour study

In this study, three representative amines, EMEA, DMEDA, and DMPDA, were selected as high-performance absorbents for CO_2 capture, based on findings from current research. The phase behaviours of the two screened green solvents (MAADMA and MOB, Table 2) blended with these three amines after absorption are summarised in Table 3. As water-lean solvents are generally focused on formulations with no more than 20 wt% water as reported in many studies[44-46], water contents of 0, 5, 10, and 15 wt% were selected in this work. Three representative sample photographs of the observed phase behaviours are shown in Figure 3, including homogeneous (a), gelation (b), and crystallization (c). No obvious liquid–liquid biphasic separation was observed under the tested conditions.

Most of the tested systems remained homogeneous after CO_2 absorption, indicating that the selected green organic solvents were generally able to maintain acceptable phase stability in the formulations. The DMEDA systems exhibited superior phase stability, with both DMEDA/MAADMA and DMEDA/MOB remaining homogeneous over the entire tested water-content range. For the EMEA systems, EMEA/MAADMA remained homogeneous, whereas EMEA/MOB underwent crystallisation at water contents of 10 and 15 wt%. For DMPDA/MAADMA, the solution remained homogeneous at 0 and 5 wt% H_2O, but gelation occurred at 10 and 15 wt% H_2O, indicating a trend of reduced phase stability at higher water contents. In contrast, DMPDA/MOB remained homogeneous throughout the entire range of water content. These results demonstrate that replacing toxic conventional organic media with greener alternatives does not necessarily compromise

phase stability. Since all tested systems exhibited homogeneous behaviour at water contents of 0 and 5 wt% and considering that most high-performance NMP-based water-lean solvents in the literature employed 5 wt% water, this specific water content was chosen for the subsequent performance evaluation. Table 4 summarizes the compositions and abbreviations of all the investigated water-lean solvents. For comparative purposes, the corresponding aqueous solvents were also investigated.

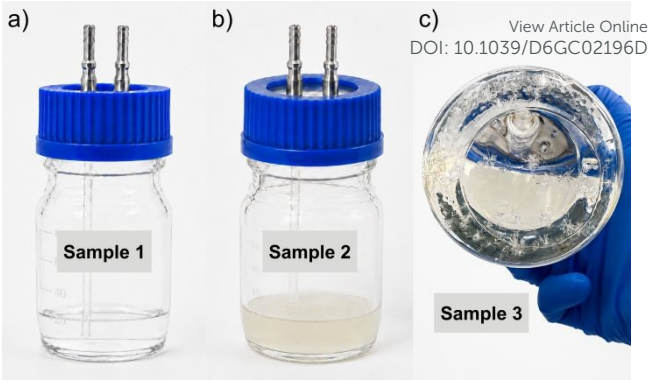

Figure 3. Representative photographs of phase behaviours after CO_2 absorption: a) homogeneous, b) gelation, and c) crystallization.

Table 3. Phase behaviour of water-lean solvents after absorption.

Amine (30 wt%)	Organic solvent	70 wt%	65 wt%	60 wt%	55 wt%
EMEA	MAADMA	Homogeneous	Homogeneous	Homogeneous	Homogeneous
	MOB	Homogeneous	Homogeneous	Crystallization	Crystallization
DMEDA	MAADMA	Homogeneous	Homogeneous	Homogeneous	Homogeneous
	MOB	Homogeneous	Homogeneous	Homogeneous	Homogeneous
DMPDA	MAADMA	Homogeneous	Homogeneous	Gelation	Gelation
	MOB	Homogeneous	Homogeneous	Homogeneous	Homogeneous

Table 4. Compositions and abbreviations of aqueous solvents and water-lean solvents studied in this work.

Abbreviation	Amine (wt%)	Cosolvent (wt%)	H_2O (wt%)
MEA	30% MEA	-	70%
EMEA	30% EMEA	-	70%
DMEDA	30% DMEDA	-	70%
DMPDA	30% DMPDA	-	70%
EM-N-5H	30% EMEA	65% NMP	5%
EM-A-5H	30% EMEA	65% MAADMA	5%
EM-O-5H	30% EMEA	65% MOB	5%
DE-N-5H	30% DMEDA	65% NMP	5%
DE-A-5H	30% DMEDA	65% MAADMA	5%
DE-O-5H	30% DMEDA	65% MOB	5%
DP-N-5H	30% DMPDA	65% NMP	5%
DP-A-5H	30% DMPDA	65% MAADMA	5%
DP-O-5H	30% DMPDA	65% MOB	5%

Absorption and desorption performance

Absorption rate. The absorption rate (r_{abs}) curves of the investigated solvents are shown in Figure 4. In general, the absorption rates of all systems declined with time as reactive amines were consumed and the driving force for CO_2 capture decreased. However, the decay behaviour differed markedly among the tested solvents.For the aqueous amine solvents, MEA displayed distinct multi-stage behaviour: an initial rapid drop, followed by a moderate region, and finally an accelerated decline. By comparison, the decrease in EMEA was more uniform during the whole process. In addition, DMEDA and DMPDA maintained relatively high rates for a longer duration, exhibiting better sustained absorption behaviour. Even in the later stages, both of them retained relatively high rates of 21 and 18 mL/min, respectively.

For the water-lean solvents, the effect of the cosolvent was evident. At identical absorption times, the solvents containing MAADMA generally showed superior rate performance compared to their MOB and NMP-based counterparts. Although some MOB systems displayed moderate initial absorption rate, the rate declined much faster. In summary, from the perspective of absorption kinetics, MOB is less effective than MAADMA in constructing high-performance green water-lean solvents.

For the effect of amine under the same cosolvent, the overall order was DMEDA > DMPDA > EMEA, suggesting that the intrinsic amine structure still played an important role even after the introduction of cosolvent. Notably, even though some solvents such as DE-N-5H and DP-N-5H exhibited high initial absorption rates, these rates declined much faster, leading to an overall unsatisfying absorption capacity performance.

Overall, during the entire absorption period, DE-A-5H, DP-A-5H and EM-A-5H showed the most favourable sustained performance, maintaining high rates for longer durations. This behaviour is desirable for practical CO_2 capture as it indicates a longer effective absorption window.

View Article Online
DOI: 10.1039/D5GC01205D

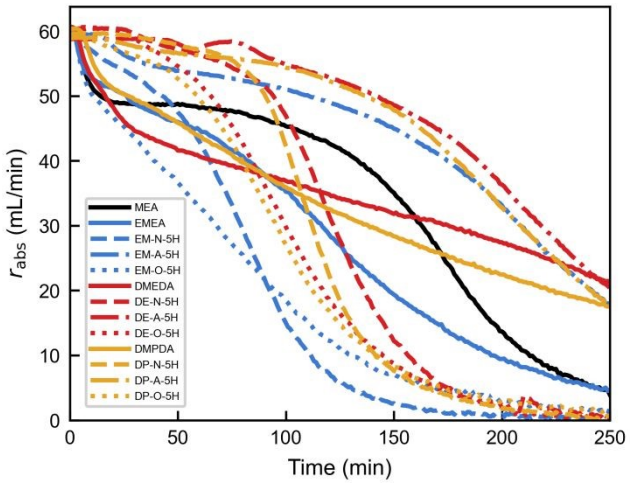

Figure 4. Absorption rate of aqueous and water-lean solvents at 313 K under a simulated flue gas (12% CO_2 and 88% N_2).

Absorption capacity. The CO_2 loading (α) changes of the tested solvents within 250-min absorption time are presented in Figure 5 and the maximum CO_2 loadings after reaching equilibrium are summarized in Figure 6. The trends in both figures are consistent, indicating that the relative differences among the solvents were well established within the 250-min timeframe.

As indicated, not all solvents can reach complete saturation within the pre-set 250 min absorption time. In particular, the aqueous DMEDA and DMPDA solvents and MAADMA-based water-lean solvents generally continued to show substantial absorption ability at the end of the test, consistent with their higher saturated loadings shown in Figure 6.

In aqueous amines, the CO_2 loading followed the order DMPDA > DMEDA > EMEA > MEA over most of the absorption period. A similar trend was observed in water-lean formulations with the same cosolvent, confirming the substantial role of amine structure in determining the absorption performance. Notably, in water-lean solvents, the choice of cosolvent had a more profound impact. DP-A-5H achieved the highest loading among all tested solvents, reaching 1.09 mol CO_2/mol amine within 250 minutes and 1.18 mol CO_2/mol amine after saturation. By contrast, DP-N-5H and DP-O-5H reached equilibrium loadings of 0.66 and 0.57, respectively in 250 minutes. DE-A-5H achieved 0.97 mol CO_2/mol amine within 250 minutes and further increased to 1.08 mol CO_2/mol amine at equilibrium, while DE-N-5H and DE-O-5H presented maximum loadings of only 0.63 and 0.52 mol CO_2/mol amine, respectively. A similar trend was observed for the EMEA-based water-lean solvents. Overall, after 250 minutes, water-lean solvents containing MAADMA exhibited 54–134% and 90–142% higher loadings than the corresponding NMP and MOB-based systems. In other words, MAADMA was markedly superior to NMP and MOB in all the three amine systems.

Importantly, all three MAADMA-based water-lean solvents exhibited higher CO_2 loadings than their corresponding aqueous amines. This is a significant finding, as water-lean solvents are often expected to exhibit lower CO_2 absorption capacity than the corresponding aqueous solvents when water is replaced by an organic cosolvent[44]. In this work, MAADMA systems overcame this limitation, delivering both greener solvent replacement and enhanced CO_2 absorption capacity.

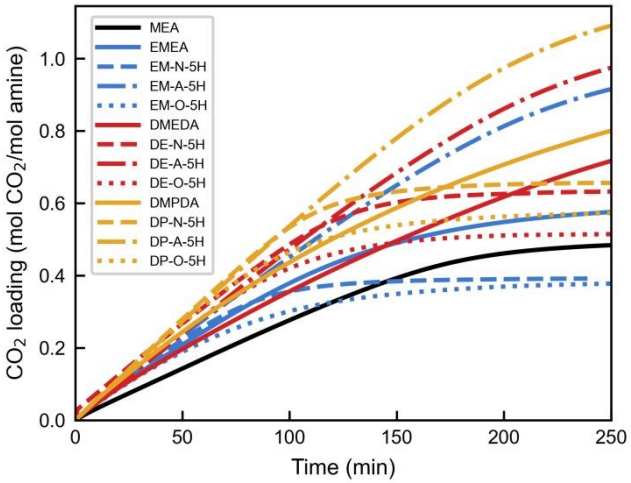

Figure 5. Absorption loading of aqueous and water-lean solvents at 313 K under a simulated flue gas (12% CO_2 and 88% N_2)

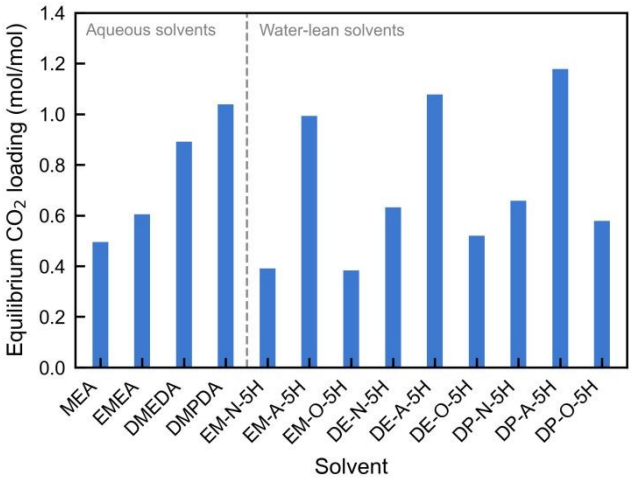

Figure 6. Equilibrium CO_2 loading of aqueous and water-lean solvents at 313 K under a simulated flue gas (12% CO_2 and 88% N_2).

Desorption performance. The desorption performance of the tested solvents was investigated, as efficient CO_2 release is essential for solvent regeneration and greatly affects the cyclic operation. As shown in Figure 7, compared to aqueous amines, all water-lean solvents exhibited faster desorption rate (r_{des}). The initial modest decrease in CO_2 loading corresponds to the heating phase, where the temperature rises towards the desorption set-point. Another notable observation is that most NMP- and MOB-based water-lean solvents approached equilibrium by the end of the 300-min desorption process. In contrast, the aqueous amines and MAADMA-based water-lean

solvents continued to exhibit certain desorption capability at 300 min. With an increasing desorption time, the advantage of the MAADMA systems became more evident. At identical time intervals, their desorption rate generally followed the order of EM-A-5H > DE-A-5H > DP-A-5H.

Despite the above findings, a high desorption rate did not necessarily translate to superior overall desorption performance. In terms of CO_2 loading, DE-A-5H and DP-A-5H showed the highest residual loadings among all solvents, at approximately 0.30 and 0.26 mol CO_2/mol amine, respectively. When comparing the effect of amine, the EMEA solvents generally achieved more complete desorption within 300 min than the other systems. In particular, the residual loadings for the EMEA water-lean solvents were as low as 0.02 mol CO_2/mol amine for EM-N-5H and EM-O-5H.

Overall, while MAADMA exhibited relatively high and sustained desorption rates, only the EMEA platform proved more conducive to achieving more thorough desorption within a reasonable duration. Consequently, the desorption behaviour is jointly determined by the organic cosolvent and the amine.

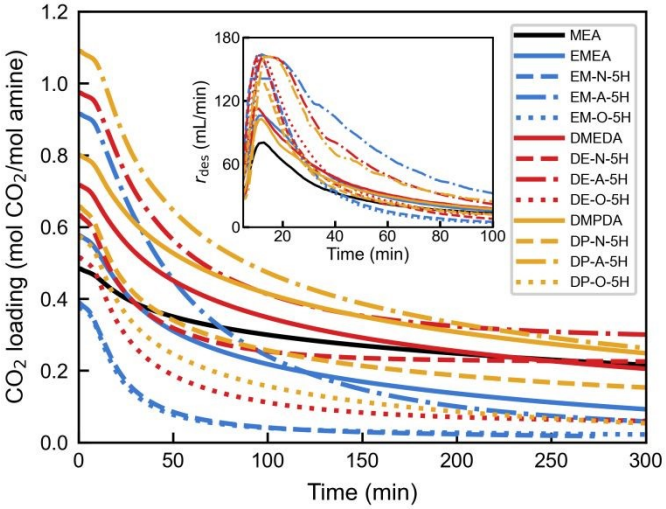

Figure 7. Desorption performance of aqueous and water-lean solvents at 353 K and atmospheric pressure.

Cyclic capacity and regeneration efficiency. The cyclic capacity and regeneration efficiency following 250 min of absorption and 300 min of desorption are shown in Figure 8. Both metrics are critical for evaluating the practical performance of solvents. In this study, cyclic capacity was determined as the difference between the CO_2-rich loading after absorption and CO_2-lean loading after desorption (i.e., $\alpha_{rich} - \alpha_{lean}$). The regeneration efficiency was calculated as the ratio of cyclic capacity to the rich loading.

Among the aqueous amine solvents, the cyclic capacity followed the order: DMPDA > DMEDA > EMEA > MEA. MEA showed the lowest regeneration efficiency at only 55%. The regeneration efficiency of DMEDA at 71% was slightly higher than that of DMPDA, whereas EMEA reached 84%, about 1.5 times that of MEA. For the water-lean solvents, the MAADMA-based systems exhibited clear advantages in cyclic capacity across all three amines. Substituting NMP with the green solvent MAADMA resulted in a significant increase in cyclic capacity: 129% for EM-A-5H relative to EM-N-5H and 66% for DE-A-5H relative to DE-N-5H. Among all tested solvents, EM-A-5H showed the highest cyclic capacity (0.86 mol CO_2/mol amine), followed by DP-A-5H (0.83 mol CO_2/mol amine).Although the MOB-based water-lean solvents showed relatively high regeneration efficiencies over 88%, their cyclic capacities remained much lower than those of the MAADMA-based ones. Notably, EMEA-based water-lean solvents exhibited the highest regeneration efficiencies, all exceeding 93%, which diminished the relative importance of MOB in enhancing the regeneration efficiency. In summary, the green replacement strategy utilizing MAADMA was highly successful in enhancing both performance metrics.

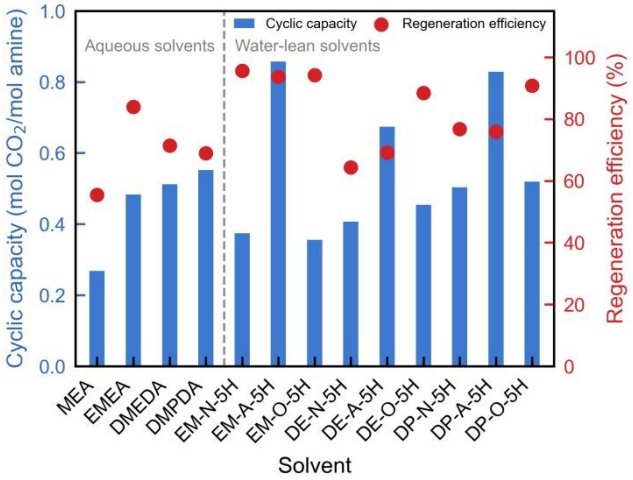

Figure 8. Cyclic capacity and regeneration efficiency of the aqueous and water-lean solvents.

Regeneration energy evaluation

Based on the results discussed above, EM-A-5H exhibited the highest cyclic capacity and the third highest regeneration efficiency. Consequently, it was selected as the representative green water-lean solvent for further regeneration energy evaluation. For a comprehensive comparison, the benchmark MEA and three high-performing NMP-based water-lean solvents were also evaluated, with the results illustrated in Figure 9.

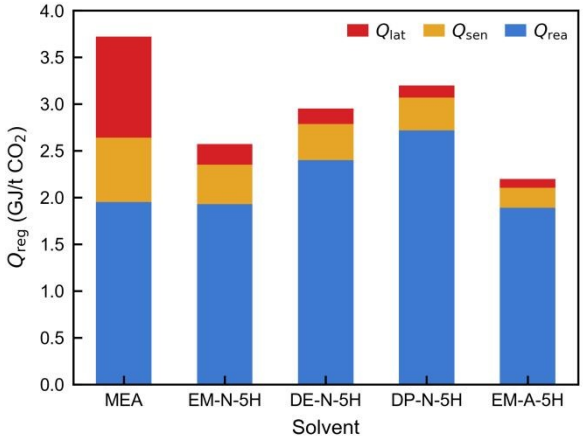

Figure 9. Comparison of the regeneration heat for EM-A-5H, aqueous MEA, and three NMP-based water-lean solvents.

As shown, the heat of absorption (Q_{rea}) constituted the largest proportion of the total regeneration heat for all tested solvents. EM-N-5H and EM-A-5H showed similar Q_{rea} values comparable to that of MEA due to their similar amine structures. In contrast, the Q_{rea} values of the other two amine-based solvents are 23% and 39% higher than MEA, respectively.

The sensible heat (Q_{sen}) of the water-lean solvents was lower than that of the aqueous MEA solution, primarily due to their lower heat capacities. Specifically, the heat capacity of aqueous MEA is around 4.0 $kJ \cdot kg^{-1} \cdot K^{-1}$, whereas those of the four water-lean solvents ranged from 2.2 to 2.8 $kJ \cdot kg^{-1} \cdot K^{-1}$. More notably, the latent heat (Q_{lat}) of the water-lean solvents was significantly lower than that of the aqueous amine solvent. This reduction is attributed to the much lower water content, which minimizes the energy penalty associated with water evaporation. Among all tested solvents, EM-A-5H achieved the lowest sensible heat (0.22 GJ/t CO_2) and lowest latent heat (0.09 GJ/t CO_2). As a result, EM-A-5H exhibited the lowest total regeneration heat at 2.20 GJ/t CO_2, representing a 41% reduction compared to that of MEA (3.72 GJ/t CO_2).

Furthermore, substituting NMP with MAADMA in the EMEA system resulted in a slight decrease in the heat of absorption, while the sensible heat and latent heat decreased much more significantly. Compared to EM-N-5H, EM-A-5H reduced the total regeneration energy by 15% following the green solvent replacement. This direct comparison further highlights the significant advantages of the green cosolvent substitution strategy.

At the molecular level, the excellent overall performance of the MAADMA–EMEA water-lean solvent can be interpreted by the altered intermolecular interactions with CO_2. First, due to the oxygen-directed hydration of its hydroxyl group, EMEA exhibits reduced water clustering around the secondary amine nitrogen, thereby improving the accessibility of the reactive site for CO_2 attack. Meanwhile, the oxygen-rich MAADMA cosolvent may further interact with residual water, disrupting the hydration shell around EMEA and accelerating CO_2 absorption[47]. Second, the low water content together with the polar ether groups of MAADMA creates a locally polar micro-environment that favors the formation of carbamic acid. Hydrogen-bonded carbamic acid clusters can stabilize the absorbed CO_2, allowing the system to achieve a higher effective loading[48]. Finally, during thermal regeneration, the polar MAADMA–water matrix may facilitate proton transfer in carbamate decomposition. The acetal oxygen sites of MAADMA are likely to assist the cleavage of the EMEA–CO_2 bond via a proton-relay mechanism, potentially lowering the activation energy for CO_2 release and thus reducing the regeneration energy[30]. Together, these molecular interactions offer a plausible explanation for the enhanced absorption and regeneration performance of the MAADMA-containing water-lean solvent.

Solvent stability demonstration

The cyclic stability of EM-A-5H was evaluated from its cyclic capacity and regeneration efficiency over 7 consecutive absorption–desorption cycles. The rich and lean loadings were obtained after 250 min absorption and 300 min desorption, respectively.

As shown in Figure 10, the EM-A-5H solvent exhibited excellent cyclic stability over 7 cycles. Although the rich and lean loadings showed slight fluctuations from cycle to cycle, these variations did not compromise the overall cyclic performance. The cyclic capacity remained nearly constant, fluctuating within a narrow range of 0.85–0.87 mol CO_2/mol amine, indicating that its working capacity was well preserved during continuous absorption–desorption cycling.

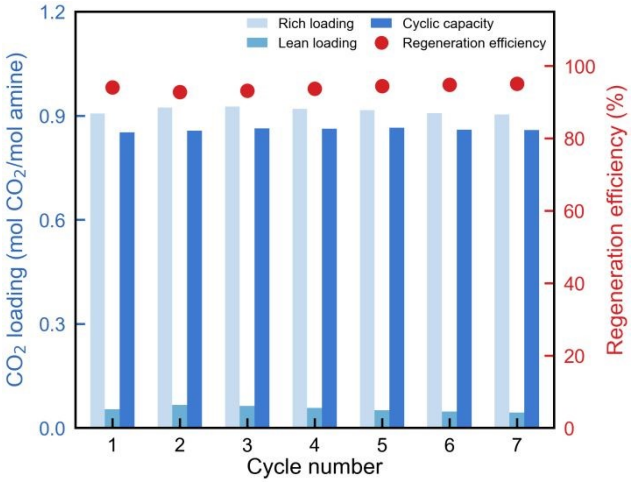

Figure 10. Continuous absorption–desorption experimental results for the EM-A-5H water-lean solvent.

The regeneration efficiency also remained high throughout the cycling test, staying close to 94% with only minor variations. These results demonstrate that EM-A-5H could effectively release most of the absorbed CO_2 during each desorption step, with stable regeneration performance over repeated use.

Coupled with its low regeneration energy consumption and environmental benignity, the EM-A-5H solvent exhibited excellent overall cyclic stability, confirming its great potential for practical CO_2 capture applications.

Viscosity and industrial applicability

In addition to stability, solvent viscosity is another key parameter determining its practical applicability. Therefore, the viscosity of EM-A-5H was further measured at different CO_2 loadings. As summarized in Table 5, the viscosity of EM-A-5H increased with CO_2 loading, from 70.34 mPa·s at a CO_2 loading of 0.87 mol CO_2/mol amine to 156.6 mPa·s at the equilibrium loading of 0.99 mol CO_2/mol amine. Notably, under a practical cyclic operating window, the solvent is generally not expected to reach full equilibrium saturation. At a loading corresponding to 90% of the equilibrium state, the viscosity remained below the commonly recognized high-viscosity threshold of 100 mPa·s for industrial depolyment[49].

Although both MAADMA and EMEA are commercially available chemical reagents, the estimated cost of EM-A-5H is higher than that of conventional aqueous amine solvents. Nevertheless, EM-A-5H is considered to have high potential for industrial application due to the following reasons. First, in industrial CO_2 capture, energy cost (i.e., operational expenditure) typically dominates the total cost, and EM-A-5H exhibited significantly lower energy consumption. Second, EM-A-5H also showed high cyclic stability, meaning that only a small amount of fresh solvent is required as makeup during long-term operation, while the majority of the solvent is recycled. Overall, EM-A-5H is a promising green CO_2 capture solvent with strong industrial applicability.

Table 5. Viscosity of EM-A-5H at different CO_2 loadings at 313 K.

CO_2 loading (mol/mol)	Viscosity (mPa·s)	Relative loading to equilibrium (%)
0.87	70.34	87.9
0.88	74.49	88.9
0.90	87.59	90.9
0.99	156.6	100.0

Conclusions

In this work, we demonstrated the feasibility of replacing the hazardous cosolvent NMP with green organic solvents in water-lean amine systems for efficient CO_2 capture. By integrating COSMO-RS-based σ-profile similarity screening with CHEM21 EHS assessments and physicochemical property filtering, MAADMA and MOB were successfully identified as promising green cosolvents from a pool of 2,562 candidates.

Comprehensive experimental evaluation revealed the great advantages of the EM-A-5H solvent (30% EMEA / 65% MAADMA / 5% H_2O), delivering a maximal cyclic capacity (0.86 mol CO_2/mol amine) and a high regeneration efficiency of 93.6%. Among all solvents experimentally evaluated herein, EM-A-5H achieved a lowest regeneration energy of 2.20 GJ/t CO_2, representing a 41% decrease compared to 30 wt% MEA and a 15% reduction over its NMP-based counterpart. Furthermore, this solvent maintained high stability over seven continuous absorption–desorption cycles without performance degradation.

The developed water-lean solvent not only addresses the critical toxicity issues of current state-of-the-art systems but also delivers superior performance, providing an efficient and sustainable alternative for industrial CO_2 capture applications.

Despite the promising results, several limitations deserve further investigation. First, the current study evaluated solvent stability over only seven absorption–desorption cycles. Longer-term testing (ideally hundreds of cycles) is necessary to fully assess solvent degradation, corrosion, and amine loss. Second, molecular-level mechanistic insights are lacking to explain the synergistic performance enhancement. *In situ* spectroscopy can be employed to elucidate the intermolecular interactions among MAADMA, amines, and CO_2 to unravel the underlying mechanisms. Third, the current solvent screening relies primarily on σ-profile similarity. Exploring alternative descriptors such as Hildebrand solubility parameters[50] and using machine learning models[51,52] could potentially accelerate the discovery of novel solvents. Finally, process-level techno-economic analysis (TEA)[53] and life-cycle assessment (LCA)[54] should be conducted to comprehensively evaluate the economic viability and environmental benefit of the proposed solvent system under realistic industrial conditions.

Author contributions

Huilin Li: Investigation; Formal analysis; Visualization; Software; Writing - Original Draft. **Xuechong Ding**: Data Curation; Validation. **Teng Zhou**: Methodology; Conceptualization; Resources; Writing - Review & Editing; Supervision; Funding acquisition.

Conflicts of interest

There are no conflicts to declare.

Data availability

All data supporting the conclusions of this paper are provided in the manuscript.

Acknowledgements

This work was supported by the Guangdong Provincial Project (2023QN10L094) and Nansha Key Science and Technology Project (2023ZD013). Teng Zhou acknowledges the financial support from the Max Planck Society through the Max Planck Partner Group Program. The authors additionally acknowledge the support from Wilson Tang Brilliant Energy Science and Technology Lab (BEST Lab) at the Hong Kong University of Science and Technology (Guangzhou).

References

1 P. Janicka, J. Płotka-Wasylka, N. Jatkowska, A. Chabowska, M. Y. Fares, V. Andruch, M. Kaykhaii and J. Gębicki, *Curr. Opin. Green Sustainable Chem.*, 2022, **37**, 100670.
2 B. A. de Marco, B. S. Rechelo, E. G. Tótoli, A. C. Kogawa and H. R. N. Salgado, *Saudi Pharm. J.*, 2019, **27**, 1-8.
3 M. A. A. Maki, K. F. Tan, M. T. S. Yee, D. K. Mishra, M. P. Venkatesh, O. W. Abduljaleel, M. Karahan and V. K. Palanirajan, *Discov. Chem.*, 2025, **2**, 342.
4 M. J. Mulvihill, E. S. Beach, J. B. Zimmerman and P. T. Anastas, *Annu. Rev. Environ. Resour.*, 2011, **36**, 271-293.
5 C. Capello, U. Fischer and K. Hungerbühler, *Green Chem.*, 2007, **9**, 927-934.
6 J. Colberg, J. L. Tucker, I. Martínez, J. D. Bailey, C. Briddell, S. G. Koenig, M. E. Kopach, S. Michalak, A. Parsons, P. F. Richardson, F. Roschangar, E. Vestergaard and A. Voutchkova-Kostal, *ACS Sustainable Chem. Eng.*, 2025, **13**, 10268-10284.

7 J. Becker, C. Manske and S. Randl, *Curr. Opin. Green Sustainable Chem.*, 2022, **33**, 100562.
8 L. Zhang, Y. Ren, W. Liu, A. Wang and T. Zhang, *Natl. Sci. Rev.*, 2018, **5**, 653-672.
9 X. Zhao, *Arab. J. Chem.*, 2026, **19**, 1882025.
10 L. Sing Soh, S. Uyin Hong, C. Zeng Liang and W. Fen Yong, *Chem. Eng. J.*, 2023, **478**, 147451.
11 A. a. F. Eftaiha, A. K. Qaroush, M. A. Abu-Daabes, H. M. Alsyouri and K. I. Assaf, *Adv. Sustainable Syst.*, 2020, **4**, 1900121.
12 M. H. Irwin, N. Gregorich, Z. Coin, R. Bhave, I. Ivanov, R. Sacci, G. Rother, D. S. Sholl and S. Z. Islam, *Chem. Eng. J.*, 2025, **525**, 169924.
13 D. Y. C. Leung, G. Caramanna and M. M. Maroto-Valer, *Renewable Sustainable Energy Rev.*, 2014, **39**, 426-443.
14 M. Wang, A. Lawal, P. Stephenson, J. Sidders and C. Ramshaw, *Chem. Eng. Res. Des.*, 2011, **89**, 1609-1624.
15 G. T. Rochelle, *Curr. Opin. Chem. Eng.*, 2012, **1**, 183-190.
16 S. Chi and G. T. Rochelle, *Ind. Eng. Chem. Res.*, 2002, **41**, 4178-4186.
17 G. Fytianos, S. Ucar, A. Grimstvedt, A. Hyldbakk, H. F. Svendsen and H. K. Knuutila, *Int. J. Greenhouse Gas Control*, 2016, **46**, 48-56.
18 W. Wu, D. Zhao, H. Liu, H. Chen, T. Liu, X. Li and Y. Deng, *Energy Fuels*, 2025, **39**, 15792-15806.
19 M. Y. Li, C. Lv, F. Zhao, L. Q. Lv, T. Fang, L. Hao, X. Dong and H. L. Liu, *AlChE J.*, 2025, **71**, e18917.
20 X. Ding, X. Li, J. Pimentel and T. Zhou, *Sep. Purif. Technol.*, 2025, **362**, 131649.
21 M. Li, X. Zhang, S. Zeng, L. Bai, H. Gao, J. Deng, Q. Yang and S. Zhang, *RSC Adv.*, 2017, **7**, 6422-6431.
22 X. Sun, S. Zeng, G. Li, Y. Bai, M. Shang, J. Zhang and X. Zhang, *AlChE J.*, 2024, **70**, e18376.
23 A. I. Papadopoulos, F. A. Perdomo, F. Tzirakis, G. Shavalieva, I. Tsivintzelis, P. Kazepidis, E. Nessi, S. Papadokonstantakis, P. Seferlis, A. Galindo, G. Jackson and C. S. Adjiman, *Chem. Eng. J.*, 2021, **420**, 127624.
24 S. Foorginezhad and X. Ji, *Sep. Purif. Technol.*, 2024, **347**, 127593.
25 S. Foorginezhad and X. Ji, *J. CO2 Util.*, 2025, **95**, 103065.
26 Y. Xu, T. Wang, Q. Yang, H. Yu, M. Fang and G. Puxty, *Chem. Eng. J.*, 2021, **425**, 131410.
27 Y. Xu, M. Fang, Q. Yang, Z. Xia, H. Yu, T. Wang, K. Chen and G. Puxty, *Greenhouse Gases:Sci. Technol.*, 2021, **11**, 828-836.
28 Z. Qi, F. Liu, H. Ding and M. Fang, *Fuel*, 2023, **350**, 128726.
29 F. Liu, Z. Qi, M. Fang and H. Ding, *Chem. Eng. J.*, 2023, **459**, 141634.
30 Y. Zhu, H. Xi, S. Zhou, M. Shreka, P. Zhou, H. Wang and W. Yang, *Chem. Eng. J.*, 2025, **518**, 164826.
31 V. Lee, J. Y. Ten, M. H. Hassim and N. G. Chemmangattuvalappil, *Proc. Integr. Optim.*, 2020, **4**, 297-308.
32 T. Zhou, Z. Qi and K. Sundmacher, *Chem. Eng. Sci.*, 2014, **115**, 177-185.
33 S. Linke, K. McBride and K. Sundmacher, *ACS Sustainable Chem. Eng.*, 2020, **8**, 10795-10811.
34 L. Y. Garcia-Chavez, A. J. Hermans, B. Schuur and A. B. de Haan, *Sep. Purif. Technol.*, 2012, **97**, 2-10.
35 L. Moity, M. Durand, A. Benazzouz, C. Pierlot, V. Molinier and J.-M. Aubry, *Green Chem.*, 2012, **14**, 1132-1145.
36 H. Zeinali, A. Mirian, H. Sameti and B. BabaAli, *Comput. Electr. Eng.*, 2015, **48**, 226-238.
37 B. Sanchez-Lengeling, L. Roch, J. D. Perea, S. Langner, C. J. Brabec and A. Aspuru-Guzik, *ChemRxiv*, 2018.
38 X. Zhang, X. Ding, Z. Song, T. Zhou and K. Sundmacher, *AlChE J.*, 2021, **67**, e17340.
39 D. Prat, A. Wells, J. Hayler, H. Sneddon, C. R. McElroy, S. Abou-Shehada and P. J. Dunn, *Green Chem.*, 2016, **18**, 288-296.
40 C. U. Mussagy, C. N. Alvarado-Holtheuer, A. Pessoa and F. O. Farias, *Sep. Purif. Technol.*, 2026, **383**, 136174.
41 Y. Shen, C. Jiang, S. Zhang, J. Chen, L. Wang and J. Chen, *Appl. Energy*, 2018, **230**, 726-733.
42 X. Zhao, X. Li, H. Lu, H. Yue, C. Liu, S. Zhong, K. Ma, S. Tang and B. Liang, *Chem. Eng. J.*, 2021, **422**, 130389.
43 A. Dreimanis, *J. Sediment. Res.*, 1962, **32**, 520-529.
44 Q. Long, S. Wang and S. Shen, *Chem. Eng. Sci.*, 2023, **273**, 118658.
45 Z. Zhang, Y. Ge, X. Heng, L. Yang, Z. Wang, F. Liu, X. Yang and K. Liu, *Energy*, 2025, **324**, 136039.
46 L. Wang, X. Wang, J. Ma, F. Meng, K. Li, M. Li, R. Wang, H. Wang, H. Gao, K. Zhao, D. Fu and P. Zhang, *Energy*, 2025, **320**, 135232.
47 N. Yu, S. Wang, M. Zhou, M. Xiao, B. Jin, H. Gao and Z. Liang, *AlChE J.*, 2026, **72**, e70260.
48 J. Leclaire, D. J. Heldebrant, K. Grubel, J. Septavaux, M. Hennebelle, E. Walter, Y. Chen, J. L. Bañuelos, D. Zhang, M.-T. Nguyen, D. Ray, S. I. Allec, D. Malhotra, W. Joo and J. King, *Nat. Chem.*, 2024, **16**, 1160-1168.
49 Z. Wang, S. He, Y. Li and S. Li, *Innovation (Camb)*, 2026, **7**, 101250.
50 J. Y. Ten, Z. H. Liew, X. Y. Oh, M. H. Hassim and N. Chemmangattuvalappil, *Proc. Integr. Optim.*, 2021, **5**, 269-284.
51 X. Liu, J. Chen, Y. Qiu, K. Xie, J. Cheng, X. You, G. Chen, Z. Song and Z. Qi, *AlChE J.*, 2025, **71**, e18631.
52 Z. Song, H. Shi, X. Zhang and T. Zhou, *Chem. Eng. Sci.*, 2020, **223**, 115752.
53 X. Ding, H. Chen, J. Li and T. Zhou, *Carbon Capture Sci. Technol.*, 2023, **9**, 100136.
54 Y. Hu, R. Gani, K. Sundmacher and T. Zhou, *Chem. Eng. Sci.*, 2024, **298**, 120423.

View Article Online
DOI: 10.1039/D6GC02196D

View Article Online
DOI: 10.1039/D6GC02196D

Data availability

All data supporting the conclusions of this paper are provided in the manuscript.